

Structure and Conformation of Individual Molecules upon Adsorption of a Mixture of Benzoporphyrins on Ag(111), Cu(111), and Cu(110) Surfaces

Rajan Adhikari,^[a] Jan Brox,^[a] Stephen Massicot,^[a] Michael Ruppel,^[b] Norbert Jux,^[b] Hubertus Marbach,^[a] and Hans-Peter Steinrück^{*[a]}

We investigated the adsorption behavior of a mixture of six 2H-tetrakis-(3, 5-di-*tert*-butylphenyl)(x)benzoporphyrins (2H-diTTBP(x)BPs, x=0, 1, 2-*cis*, 2-*trans*, 3, and 4) on Ag(111), Cu(111) and Cu(110) at room temperature by scanning tunneling microscopy (STM) under ultra-high vacuum conditions. On Ag(111), we observe an ordered two-dimensional square phase, which is stable up to 400 K. On Cu(111), the same square phase coexists with a stripe phase, which disappears at 400 K. In contrast, on Cu(110), 2H-diTTBP(x)BPs adsorb as immobile isolated molecules or dispersed short chains along the [110] substrate direction, which remain intact up to 450 K. The stabilization of the 2D supramolecular structures on

Ag(111) and Cu(111), and of the 1D short chains on Cu(110) is attributed to van der Waals interactions between the *tert*-butyl and phenyl groups of neighboring molecules. From high-resolution STM, we can assign all six 2H-diTTBP(x)BPs within the ordered structures. Moreover, we deduce a crown shape quadratic conformation on Ag(111) and Cu(111), an additional saddle-shape on Cu(111), and an inverted structure and a quadratic appearance on Cu(110). The different conformations are attributed to the different degree of interaction of the iminic nitrogen atoms of the isoindole and pyrrole groups with the substrate atoms.

Introduction

The organization of matter at the molecular or even atomic level is still a difficult task. The goal is to develop molecular scale devices, that is, devices that contain a single molecule or molecular assembly embedded as a key component,^[1] which not only meet the increasing technical demands of the miniaturization of conventional Si-based electronic devices but also offers an ideal window of exploring the inherent properties of materials at the molecular level. In order to realize, e.g., molecular scale electronic devices from organic building blocks, one has to control and characterize the adsorption and arrangement of molecular nanostructures on suitable substrates with high precision. To enable the fabrication of nanometer-size structures, significant efforts have been made to develop the

fundamental understanding of the adsorption and properties of functional organic molecules on various substrates.^[2] Investigation of the different self-assembled structures of the molecules on surfaces is of fundamental importance, because the physical and chemical properties of the various molecular assemblies depend on their structures and conformations.^[3] Additionally, in a molecular device, the conformation of the molecule at the interface is key.^[1a,4] The molecule should not lose its functionality, or else, the device may not function. Many studies have been performed using scanning tunneling microscopy (STM), which opens up the possibility to directly investigate and/or identify the conformation of individual molecules, such as porphyrins,^[2d,5] in their adsorbed states on single crystal coinage metal surfaces.

Among the class of nitrogen-containing macrocycles, porphyrins are omnipresent in nature^[6] and are most exploited representatives, in part because of their significance to biology.^[7] They are an essential building block of living systems, e.g., for oxygen transport in mammals and photosynthesis. Their unique electronic and magnetic characteristics have led to manifold applications in a variety of electronic devices.^[8] The ideal conformation of a porphyrin has D₄ symmetry, but due to the inherent flexibility of the porphyrin macrocycle, the conformation of a porphyrin can be customized by the interactions with substrates,^[2b,c] substitution with particular functional end groups,^[3c,9] molecular coverage,^[10] heat treatments,^[2b,11] presence (metalation) or absence of metal center,^[3a,9a,12] which also further alters porphyrin's adsorption behavior as well as its physical and chemical nature.

Porphyrins and phthalocyanines adsorbed on metal surfaces have so far received extensive attention within the category of

[a] R. Adhikari, Dr. J. Brox, S. Massicot, Dr. H. Marbach, Prof. Dr. H.-P. Steinrück
Lehrstuhl für Physikalische Chemie II
Friedrich-Alexander-Universität Erlangen-Nürnberg
Egerlandstr. 3, 91058 Erlangen, Germany
E-mail: hans-peter.steinrueck@fau.de
Homepage: <https://chemie.nat.fau.de/ak-steinrueck/>

[b] Dr. M. Ruppel, Prof. Dr. N. Jux
Lehrstuhl für Organische Chemie II
Friedrich-Alexander-Universität Erlangen-Nürnberg
Nikolaus-Fiebiger-Str. 10, 91058 Erlangen, Germany

 Supporting information for this article is available on the WWW under <https://doi.org/10.1002/cphc.202300355>

 © 2023 The Authors. ChemPhysChem published by Wiley-VCH GmbH. This is an open access article under the terms of the Creative Commons Attribution Non-Commercial NoDerivs License, which permits use and distribution in any medium, provided the original work is properly cited, the use is non-commercial and no modifications or adaptations are made.

nitrogen-containing macrocycles.^[13] Tetraannulated derivatives, in particular tetrabenzoporphyrins,^[14] represent an intriguing class of π -extended tetrapyrroles, due to their intermediate position between regular porphyrins and phthalocyanines. Benzoporphyrins have a variety of potential practical applications, such as organic near-infrared devices,^[15] oxygen sensors,^[16] photodynamic therapy,^[17] organic thin-film transistors,^[18] and dye-sensitized solar cells.^[14,19] Despite this relevance, only very few investigations of their adsorption behavior on different metal surfaces have been reported to date.^[20] For 2H-5,10,15,20-tetrakis-(2-naphthyl)-benzoporphyrin (2H-TNBP) on Cu(111), individual molecules were observed, whereas islands with square arrangements were observed on Ag(111);^[20a] for 2H-5,10,15,20-tetrakis(4-cyanophenyl)-tetrabenzoporphyrin (2H-TCNPTBP), Kagome, quadratic lattice, and hexagonal networks coexist on Cu(111);^[20b] for 2H-5,10,15,20-tetraphenyltetrabenzoporphyrin (2H-TPTBP), 2D islands with the molecules arranged in a herringbone structure are found on Cu(111) and Ag(111), whereas on Cu(110) 1D molecular chains were observed;^[20c] for Ni(II)-5, 10, 15, 20-tetraphenyltetrabenzoporphyrin (Ni-TPBP), oblique, herringbone, and cross structures coexist on Cu(111);^[20d] and finally for Ni(II)-meso-tetrakis(4-*tert*-butylphenyl)-benzoporphyrin (Ni-TTBPBP), islands with square arrangement were observed on Cu(111).^[20e] Such arrangements

could find potential applications in organic electronics or catalysis.

Regardless of these promising properties, research on tetrabenzoporphyrins is still only at the beginning, in particular concerning their structural diversity and the resulting properties on different surfaces. This is particularly true, since the synthesis of functionalized isolated benzoporphyrin derivatives is very challenging. Ruppel et al.^[21] reported a synthetic protocol with a library of 30 functionalized A4-symmetric tetraaryl-tetrabenzoporphyrins (TATBPs) utilizing a readily established 2H-isoindole synthon. It provides quick access to a library of different molecules; however, the separation of statistical mixtures is frequently difficult and challenging.^[21-22] For the synthesis of here studied molecules, 2H-tetrakis-(3, 5-di-*tert*-butylphenyl)(*x*)benzoporphyrins (2H-diTTBP(*x*)BPs), a mixed condensation of pyrrole and the 2H-isoindole synthon with 3,5-di-*tert*-butylbenzaldehyde were used, yielding a mixture of six different porphyrin species; thereby "*x*" indicates the number of isoindole groups (also denoted as benzopyrrole groups) in the different porphyrins. Figure 1 shows the chemical structures of the six 2H-diTTBP(*x*)BPs. The synthesis and characterization of the mixture of the 2H-diTTBP(*x*)BP molecules was done in an analogous way as has been described by Ruppel et al.^[21] elsewhere.

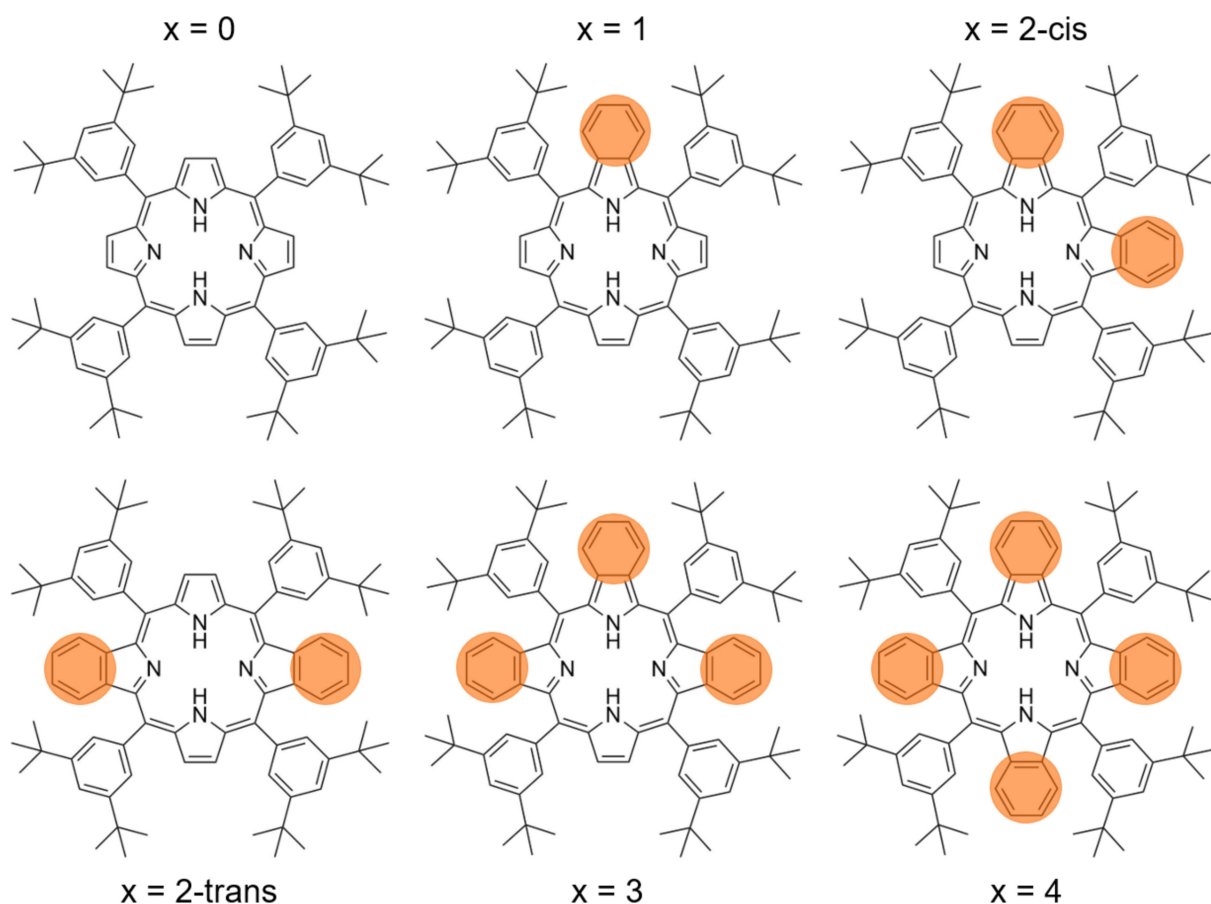


Figure 1. Chemical structure of the different 2H-diTTBP(*x*)BPs.

Herein, we present a detailed investigation of the self-assembly of 2H-diTTBP(x)BPs on Ag(111), Cu(111) and Cu(110) as a function of temperature to provide further information on fundamental aspects. While the different molecules cannot be separated in the synthesis process, we were able to identify and/or assign all six porphyrin species within the long-range ordered structures on Ag(111) and Cu(111) based on our submolecular resolution STM images. These long-range ordered structures are stabilized by van der Waals forces between the adjacent *tert*-butyl groups of neighboring molecules. On /bk; Cu(110), however, we evidence for the first time, to the best of our knowledge, a peculiar “inverted” adsorption geometry^[23] for any benzoporphyrin derivative.

Results and Discussion

2H-diTTBP(x)BPs on Ag(111)

In a first step, we investigated the adsorption behavior of 2H-diTTBP(x)BPs on Ag(111), a substrate which is considered as rather inert and does not tend to exhibit strong interactions

with metal-free porphyrins, as deduced from STM.^[12,25] Sub-monolayer coverage porphyrin films (total surface coverage of ~50%) were deposited onto the sample at RT, and the measurements were carried out also at RT. In addition, the sample was annealed to 400 K, and the subsequent STM measurements were again performed at RT.

Figure 2a shows the images measured after the deposition at RT. The overview image (left) and close-up image (middle), displays a very regular, monomodal 2D island, with nearly perfect long-range order and only very few defects. The high-resolution STM image in Figure 2a (right) shows that the phase is characterized by a square unit cell ($\gamma = 89 \pm 3^\circ$), with unit cell lattice vectors $\vec{a} = 1.56 \pm 0.10$ nm and $\vec{b} = 1.46 \pm 0.10$ nm, and a unit cell area of 2.28 nm². We propose that the unit cell contains one molecule, yielding a density of 0.44 molecules/nm². As mentioned above, the deposited 2H-diTTBP(x)BPs mixture contains six different molecules, containing 0, 1, 2 (cis and trans), 3, or 4 isoindole groups (see Figure 1). From the detailed inspection of the high-resolution STM image in Figure 2 (right), we are indeed able to identify and assign all six molecules, which are marked with differently colored dashed circles. Each individual molecule can be identified by four characteristic

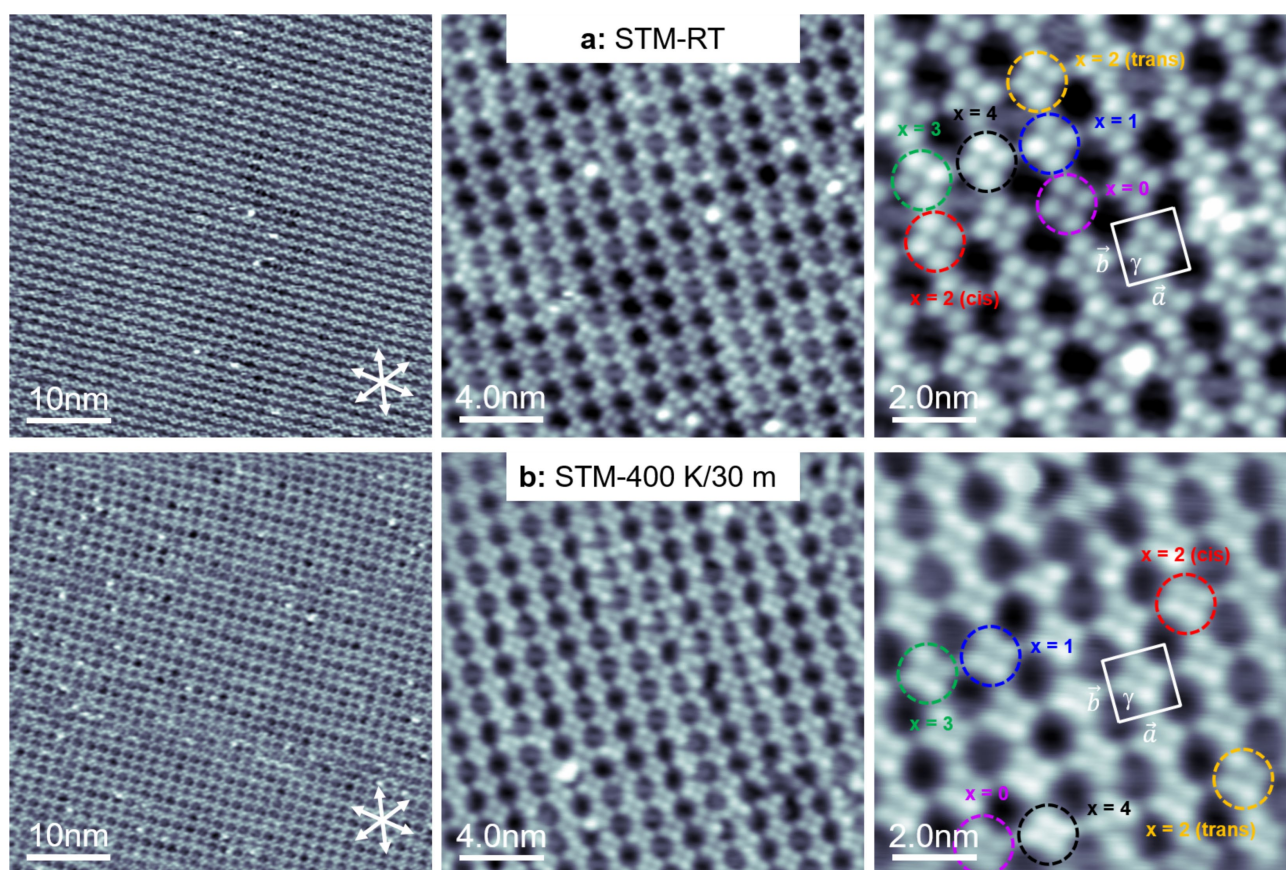


Figure 2. STM images of 2H-diTTBP(x)BPs on Ag(111), as overview (left, 50×50 nm²), close-up (middle, 20×20 nm²), and with high resolution (right, 10×10 nm²), measured at RT. a) Deposition at RT reveals a highly ordered long-range square phase. b) After annealing to 400 K for 30 min no changes are observed; the middle and right image in (b) are an average frame of 6 and 20 consecutive images, respectively. In the high-resolution images, the six different molecules ($x=0, 1, 2$ -cis, 2 -trans, 3 , & 4) can be identified and are marked with dashed colored circles. The unit cells are shown as solid white lines, and the white arrows indicate the close-packed Ag(111) substrate directions. For more details, see text. The STM images were measured with U_{bias} between 1.0 and 1.88 V and I_{set} between 89.3 and 201 pA; for details see Table S1 in the Supporting Information.

lobes, that is, bright or dim protrusions that correspond to the isoindole groups. This appearance is attributed to a “crown-shape” conformation,^[20d] which results from a subtle balance between molecule-substrate interactions and repulsive forces within the molecules. We will address the details of the intramolecular conformation later on in Figure 3.

Typically, the subtle balance between molecule-molecule and molecule-substrate interactions determines the adsorption behavior of porphyrins and other large organic molecules. On Ag(111), supramolecular arrangements of 2H-tetraphenylporphyrin (2H-TPP) are formed as a result of T-shaped intermolecular interactions between the peripheral phenyl substituents of neighboring molecules.^[25a,26] In contrast, due to strong molecule-substrate interaction between the iminic nitrogen atoms of the porphyrin and the Cu atoms of the substrate, individual 2H-TPP molecules were observed on Cu(111) at RT.^[27] For 2H-diTTBP(x)BPs on Ag(111), we do not expect site-specific molecule-substrate interactions, which would yield such immobilized isolated molecules. Furthermore, the observed long-range supramolecular arrangement is also not compatible with the commonly observed T-shaped and π - π intermolecular stacking of a similar porphyrin derivative, that is, 2H-TPTBP on Ag(111), Cu(111) and Cu(110).^[20c] Thus, we propose that the formation and lateral stabilization of the long-range ordered supramolecular arrangement observed in Figure 2a are driven by intermolecular interactions between neighboring molecules, which are mainly mediated via van der Waals forces between the *tert*-butyl groups and possibly phenyl groups of neighboring molecules.

To probe the stability of the phase, we annealed the deposited porphyrin films to 400 K for 30 min. Figure 2b shows the corresponding images after this annealing step, measured at RT. We again observe a very regular, monomodal 2D island, with nearly perfect long-range order and only very few defects. The high-resolution STM image in Figure 2b (right) shows an (within the experimental uncertainty) identical square lattice ($\gamma = 92 \pm 3^\circ$), with lattice vectors $\vec{a} = 1.56 \pm 0.10$ nm and $\vec{b} = 1.46 \pm 0.10$ nm, and a unit cell area of 2.28 nm². Assuming one molecule per unit cell, we obtain an identical density of 0.44 molecules/nm² as for the layer measured directly after deposition at RT. Again, we were able to identify all six 2H-diTTBP(x)BPs (with $x=0, 1, 2$ -cis, 2-trans, 3, and 4 isoindole groups), which are marked with colored dashed circles in the high-resolution STM image in Figure 2b (for details see Figure 3 below). Overall, the STM images in Figure 2b show that the long-range ordered monomodal 2D phase remains unchanged and is thus thermodynamically stable at 400 K.

To obtain further insight, we analyze the appearance of the individual 2H-diTTBP(x)BP molecules in more detail. Figure 3a and 3c show enlarged cutouts of the different molecules indicated in Figure 2a (RT) and Figure 2b (400 K), respectively. Each appears as four quadratically arranged, clearly identifiable bright or dim protrusions, which are separated by ~ 6 Å. Generally, a subtle balance between molecule-molecule and molecule-substrate interactions as well as steric forces within the molecule determine the intramolecular conformation of TPPs on a surface. For many porphyrins and slightly modified

TPPs, the “saddle-shape” conformation is the well-established conformation.^[20,25a,26,27b,28] However, this intramolecular conformation is not compatible with the observation of four quadratically arranged protrusions observed for the molecules on Ag(111) studied here. Thus, we need to consider a different intramolecular conformation. Interestingly, the observed peculiar appearance is very similar to that observed by Lepper et al. for Ni(II)-5, 10, 15, 20-tetraphenyltetrabenzoporphyrin (Ni-TPBP) on Cu(111).^[20d] They assign the quadratic appearance of the molecule to four upward bent isoindole groups, which appear as four bright protrusions in STM, separated by ~ 6 Å. The suggested structure is conceivable when an attractive substrate-molecule interaction pulls the macrocycle towards the substrate, increasing the tilting value of isoindole groups due to steric repulsion of the ortho-substituents within the molecule.

The proposed scaled molecular models for each of the 2H-diTTBP(x)BPs molecules on Ag(111) are depicted in Figure 3b, with the upward bent isoindole groups colored in orange, and the upward bent pyrrole groups in yellow. Due to their larger size, the isoindole groups are assigned to the bright protrusion and the pyrrole groups to the dim protrusions. The six individual 2H-diTTBP(x)BPs ($x=0, 1, 2$ -cis, 2-trans, 3, and 4) are labeled with different colors (rectangular frame) and are displayed from bottom to top: A molecule with four dim lobes is assigned to $x=0$ (violet); one bright lobe and three dim lobes are assigned to $x=1$ (blue); two bright lobes and two dim lobes are assigned to $x=2$ (cis; red) or $x=2$ (trans; orange); three bright lobes and one dim lobe are assigned to $x=3$ (green); and finally, four bright lobes are assigned to $x=4$ (black).

Overall, our proposed models are in line with the interpretation of Lepper et al.,^[20d] and the *tert*-butyl groups are nearly parallel to the surface in this geometry. In accordance with the suggested molecular geometry, the attractive interaction is due to van der Waals forces between the extended π -systems of the *tert*-butyl groups and the macrocycle of the molecule and the Ag substrate. The similarity of the appearances of 2H-diTTBP(x)BPs molecules on Ag(111) and Ni(II)-TPBP indicates that the overall conformation of the molecules within the ordered layer is not significantly influenced by presence of the *tert*-butyl groups or by the presence of a metal ion instead of two hydrogen atoms, similar to the observations for 2H-TPP and M^{2+} -TPPs.^[25a,27a]

2H-diTTBP(x)BPs on Cu(111)

To gain deeper insight into the adsorption behavior of 2H-diTTBP(x)BPs, we also investigated their properties on Cu(111). Considering the well-established differences in the adsorption behavior of 2H-TPP on Cu(111) and Ag(111),^[25a,27b] we expect a substantially different adsorption behavior or conformation also for 2H-diTTBP(x)BPs on the two surfaces. This is because Cu(111) is generally considered as a more reactive surface than Ag(111), in particular concerning N-containing molecules. Sub-monolayer coverage porphyrin films (total surface coverage of $\sim 50\%$) were deposited onto a sample at RT, and measurements were carried out also at RT, before the sample was annealed to 400

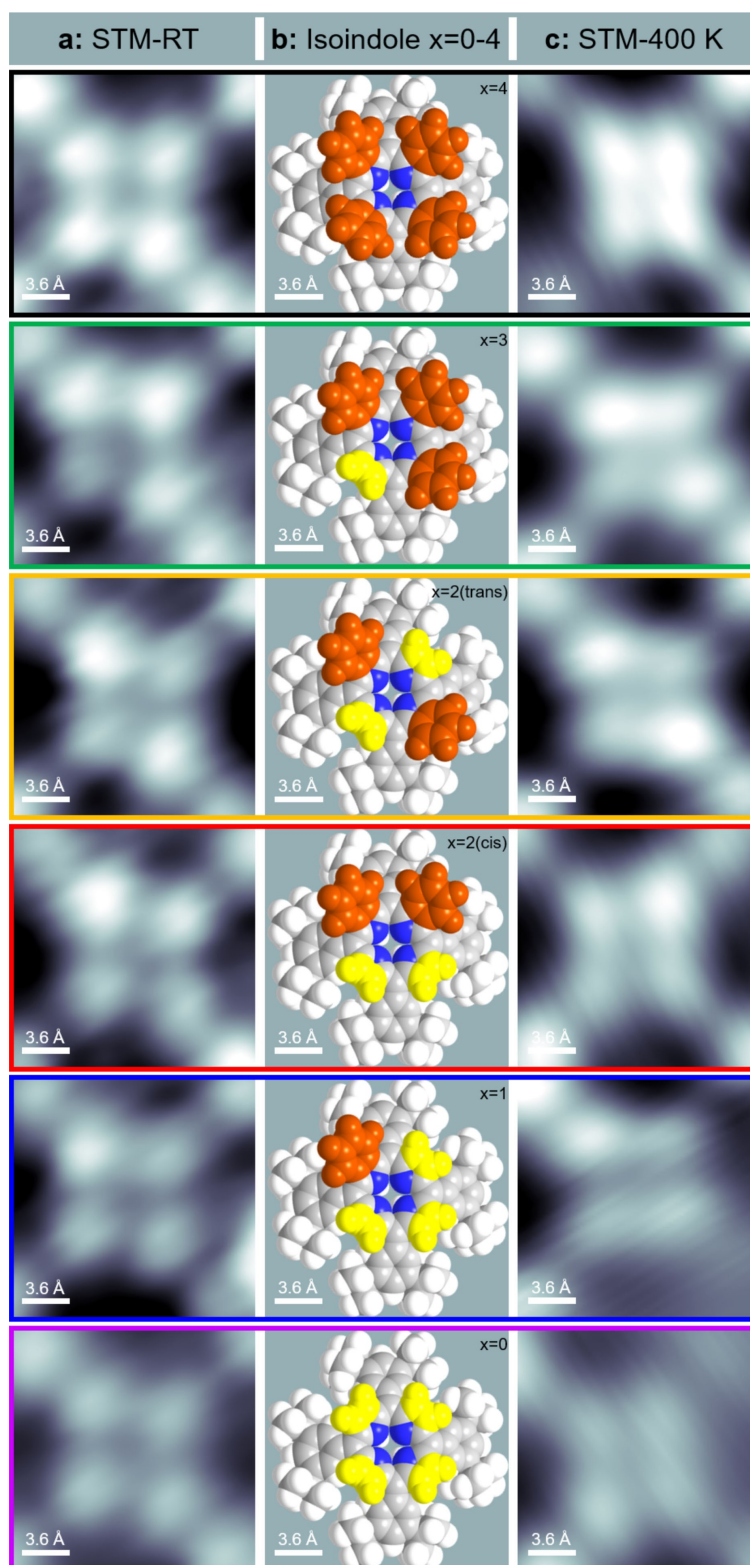


Figure 3. STM images ($1.8 \times 1.8 \text{ nm}^2$) of 2H-diTTBP(x)BPs on Ag(111) after a) adsorption at RT - cutout from Figure 2a-right, and c) after annealing to 400 K for 30 min - cutout from Figure 2b-right. Each molecule is characterized by four bright or dim protrusions. b) Scaled molecular models of the six individual molecules ($x = 0, 1, 2\text{-cis}, 2\text{-trans}, 3, \& 4$). The proposed molecular model represents a “crown-shape” conformation: Upward bent isoindole groups are depicted in orange and correspond to bright protrusions in (a) and (c); upward bent pyrrole groups are depicted in yellow and correspond to dim protrusions. The six individual molecules are marked with differently colored frames, with the same color code as used in Figure 2; for more details, see text. The STM images were measured with $U_{bias} = 1.88 \text{ V}$ and $I_{set} = 89.3$ or 201 pA ; for details see Table S1.

or 450 K to investigate the role of temperature. After each annealing step, STM was performed at RT.

Figure 4a shows the STM images after the deposition at RT (for a more extensive data set see Figure S1 in the SI). In the overview image (left), one can clearly distinguish two different self-assembled molecular ordering patterns, namely a square phase and a stripe phase, marked with white and yellow dashed lines, respectively. These structures coexist on the surface, establishing a polymorphism of the adsorbate system. The

ordered islands often grow from step edges onto the terraces, which leads us to suggest that the steps are energetically favored adsorption sites, which also act as nucleation centers for island growth.^[2c] The two phases cover about similar surface areas, which suggests a comparable adsorption energy. Between the ordered islands, a disordered phase exists, and noisy streaks are visible in the fast-scanning direction of the STM, indicating the existence of mobile molecules on the surface. This streaky appearance is ascribed to molecules moving too

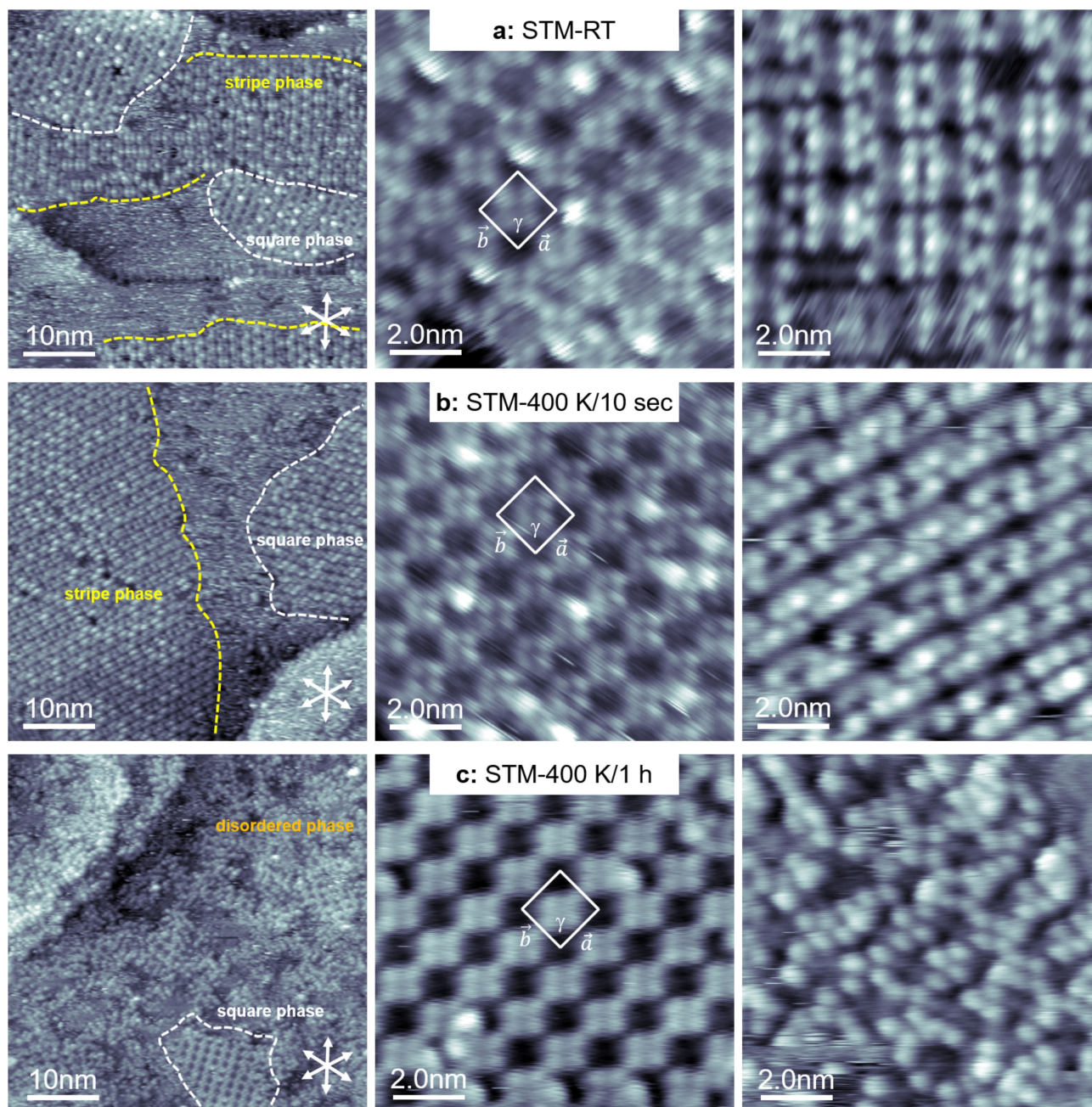


Figure 4. STM images of 2H-diTTBP(x)BPs on Cu(111), as overview (left, $50 \times 50 \text{ nm}^2$) and with high resolution (middle, right, $10 \times 10 \text{ nm}^2$), measured at RT. a) Deposition at RT reveals a coexistence of ordered square and stripe phases, along with a disordered phase. b) After annealing at 400 K for 10 sec no changes are observed. c) After further annealing at 400 K for 1 h, a loss of the stripe phase is found leaving the square phase and a disordered phase on the surface. The unit cells are shown as solid white lines, and the white arrows indicate the close-packed Cu(111) substrate directions. For more details, see text. The STM images were measured with U_{bias} between -1.59 and $+1.26$ V and I_{set} between 95.7 and 299 pA; for details see Table S1.

fast to be imaged by STM, which is in line with a two-dimensional (2D) gas phase.^[25a,27a,29]

Figure 4a (middle) shows high resolution images of the phase with the square lattice ($\gamma = 93 \pm 4^\circ$), with unit cell lattice vectors $\vec{a} = 1.48 \pm 0.10$ nm and $\vec{b} = 1.60 \pm 0.12$ nm. These values yield a unit cell area of 2.37 nm², and – with one molecule per unit cell – a density of 0.42 molecules/nm². Notably these parameters are, within the experimental uncertainty, identical to those observed above for 2H-diTTBP(x)BPs on Ag(111). The second island type, the stripe phase in Figure 4a (right), also displays a densely packed, locally ordered structure. However, due to the absence of a well-defined long-range order, it is not possible to provide a unit cell. The phase consists of molecular rows, which are perfectly aligned along the high symmetry directions of the substrate. This is particularly evident from Figure 5, where three different domains, rotated by each other by 120° , are depicted. The perfect alignment and the absence of any moiré pattern is a strong indication that the stripe phase is commensurate with the underlying substrate. The driving force likely is that the molecules have a well-defined adsorption site on the Cu(111) surface.

To gain additional insight, we discuss the appearance of individual 2H-diTTBP(x)BPs molecules within the square and the stripe phase in Figure 4 and Figure S1. In the high-resolution

image of the square phase obtained after heating to 400 K in Figure S2 (left), we were able to identify some of the 2H-diTTBP(x)BPs, that is, those with $x=0$, 2-cis, and 4. These individual molecules are denoted again by colored dashed circles, with the same color code used as for Ag(111) in Figure 3. Due to the lower resolution of the STM image (likely caused by a different STM tip termination), we were unable to identify and assign all of the six different porphyrin species. In the enlarged cutouts in Figure S2 (right; top row), the molecules appear as four, clearly identifiable bright or dim protrusions separated by ~ 6 Å. The proposed scaled molecular models are overlaid and depicted in Figure S2 (right; bottom row), using the same color code for the rectangular frame. The overall intramolecular conformation is in line with the findings on Ag(111) that were discussed in detail above.

We next discuss the appearance of individual 2H-diTTBP(x)BPs within the stripe phase depicted in Figure 6 (top). Note that in contrast to the situation for the square phase on Ag(111) in Figure 3 and on Cu(111) in Figure S2, where the molecules all had a quadratic appearance with 4 protrusions, we here observe a rectangular appearance with 6 protrusions for stripe phase. Nevertheless, we are again able to assign the different appearances to different 2H-diTTBP(x)BPs molecules, if we now assume an intramolecular structure with a saddle-

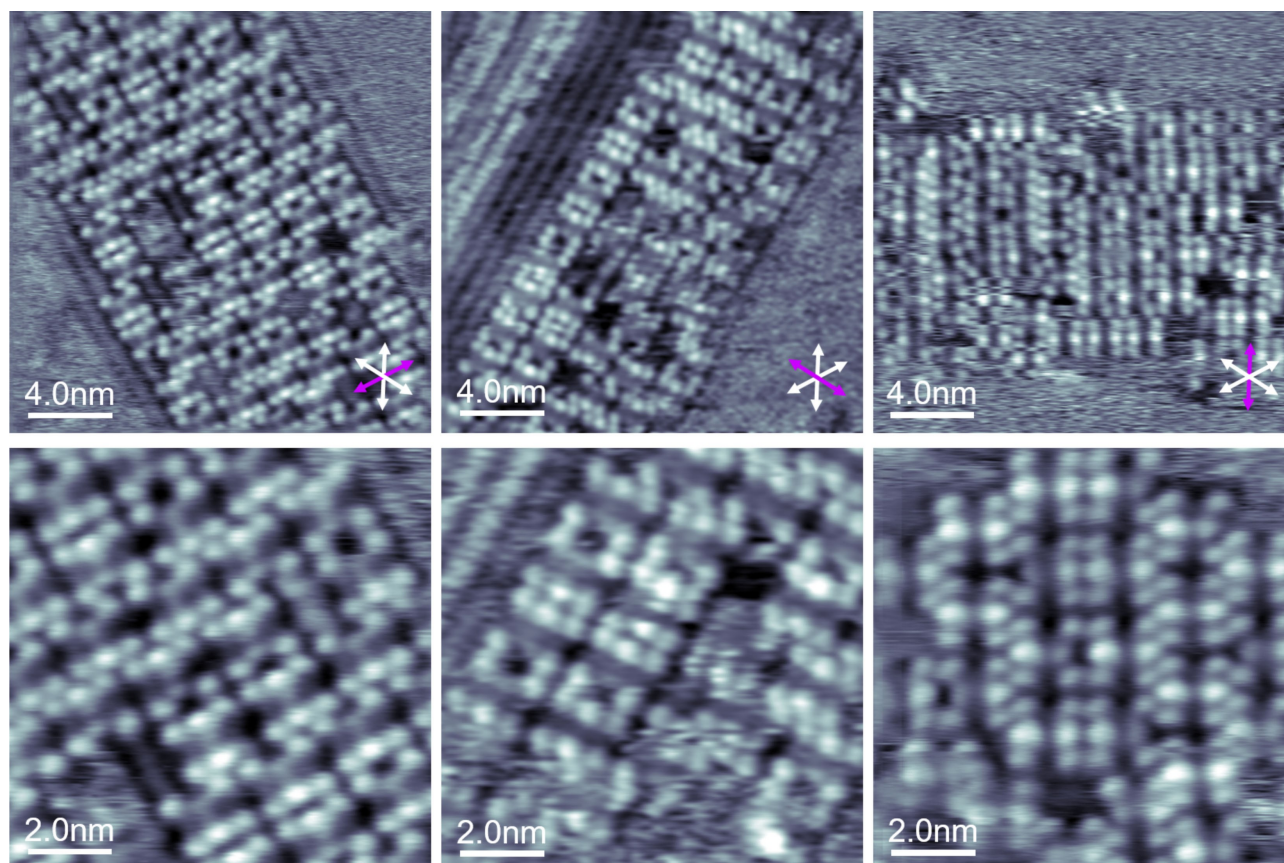


Figure 5. STM images of the stripe phase of 2H-diTTBP(x)BPs on Cu(111) measured at RT, as overview (top, 20×20 nm²) and with high resolution (bottom, 10×10 nm²). The white arrows indicate the close-packed Cu(111) substrate directions. The stripe phase was found aligned along all high symmetry axes (marked with purple arrow). For more details, see text. The STM images were measured with $U_{\text{bias}} = -1.0$ V and I_{set} between 293 and 298 pA; for details see Table S1.

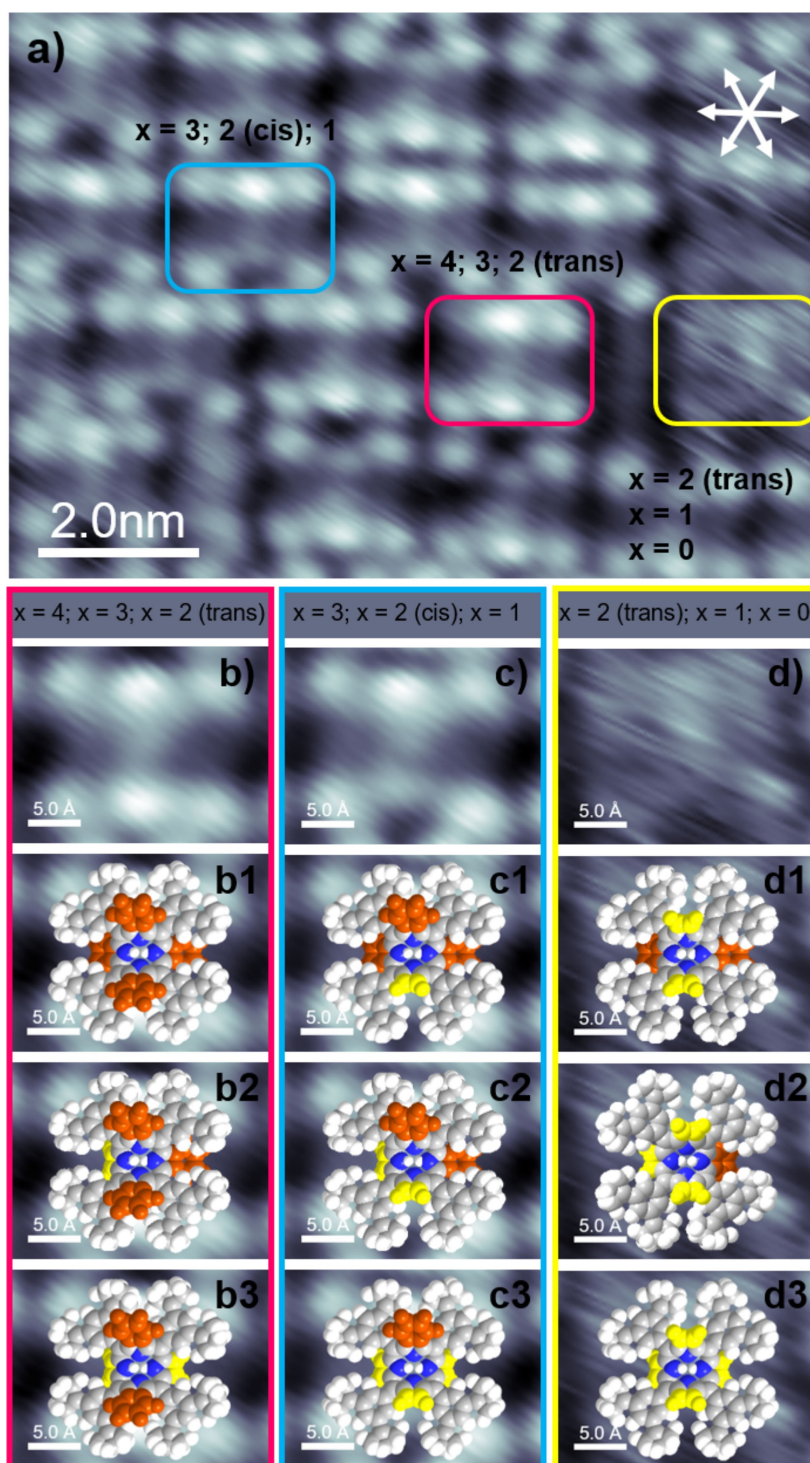


Figure 6. a) STM image of the stripe phase of 2H-diTTBP(x)BPs on Cu(111) measured at RT with high resolution (top, $10 \times 7 \text{ nm}^2$; for details see also Figure 4a,b and Figure 5). b–d) Cutouts ($2.5 \times 1.87 \text{ nm}^2$) overlaid with proposed scaled molecular models. Each molecule displays six protrusions: the outer four are assigned to the peripheral phenyl substituents, and the two central ones to the slightly bent up isoindole or pyrrole groups. The elongated depression (dark line) between two parallel groups of three protrusions is referred to as molecular axis. The proposed molecular model represents a “saddle-shape” conformation with upward/downward bent isoindole groups depicted in orange and pyrrole groups in yellow. Three different appearances are observed with TWO bright protrusions (b1–b3: red frame; $x=4, 3, \text{ or } 2$ -trans), ONE bright protrusion (c1–c3: blue frame; $x=3, 2$ -cis, or 1), and ZERO bright protrusions (d1–d3: yellow frame; $x=2$ -trans, 1, or 0). For more details, see text. The STM image were measured with $U_{\text{bias}} = -1.0 \text{ V}$, $I_{\text{set}} = 296 \text{ pA}$; for details see Table S1.

shape. Thereby, two of the isoindole or pyrrole groups are bent upward and two are bent downward. In Figure 6 (top) we

observe 3 different appearances which are indicated by differently colored rounded-edge rectangles, which all display 6

protrusions. The elongated depression (dark line) between two parallel groups of three protrusions is referred to as molecular axis; it is aligned, that is, parallel to one of the high-symmetry crystallographic directions of the Cu(111) substrate.

The outer four protrusions, that is, those at the edges of the rectangle always appear dim. By comparison with the chemical structure in Figure 1 and STM reports concerning different porphyrins in literature (see ref.^[20a,b,25a,27b] and references therein), we assign them to the peripheral phenyl substituents. The two central protrusions appear either as bright or as dim, and are assigned to the slightly upward bent isoindole or pyrrole of the saddle-shaped molecule; this is evident from Figure 6 (bottom columns, b–d), where enlarged cutouts of the STM image from Figure 6a are overlaid with a scaled molecule models. Thereby, upward bent isoindole groups are colored orange, while upward bent pyrrole groups are colored yellow.

Altogether, we can identify 3 different appearances in Figure 6. TWO bright central protrusions (red frame) are assigned to $x=4$ (b1), with two upward and two downward bent isoindole groups, or to $x=3$ (b2), with two upward bent isoindole groups and downward bent isoindole and pyrrole groups, or to $x=2$ -trans (b3), with two upward bent isoindole groups and two downward bent pyrrole groups. Appearances with ONE bright central protrusion (blue frame) are assigned to $x=3$ (c1), with upward bent isoindole and pyrrole groups and two downward bent isoindole groups, or to $x=2$ -cis (c2), with upward bent isoindole and pyrrole groups, and downward bent isoindole and pyrrole groups, or to $x=1$ (c3), with upward bent isoindole and pyrrole groups and two downward bent pyrrole groups. Appearances with ZERO bright central protrusions (yellow frame) are assigned to $x=2$ -trans (d1), with two upward bent pyrrole groups and two downward bent isoindole groups, or to $x=1$ (d2), with two upward bent pyrrole groups and downward bent isoindole and pyrrole groups, or to $x=0$ (d3), with two upward bent and two downward bent pyrrole groups.

After discussing the intramolecular conformations, we address the intermolecular interactions. For TPPs, the supramolecular arrangement is stabilized by T-shaped interactions between the phenyl rings of the neighboring porphyrins. Thereby, each phenyl group points directly to the center of a phenyl group of a neighboring molecule. Since in 2H-diTTBP(x)BPs two *tert*-butyl groups are attached to the 3- and 5-position of the phenyl groups, neither T-shaped interactions nor π - π intermolecular stacking can occur. We instead propose that the formation and lateral stabilization of the observed supramolecular arrangements are mainly mediated via van der Waals forces between the *tert*-butyl groups and possibly phenyl groups of neighboring molecules.^[20e,30] Furthermore, the overall intermolecular theme is consistent with the findings on the Ag(111) surface discussed above. The observation of the same square phase of the mixture of 2H-diTTBP(x)BPs on both surfaces indicates that the long-range order of this phase is predominantly stabilized by the outer periphery of the molecules and not by the substrate or the number of isoindole groups.

To probe the stability of the phases, we annealed the deposited porphyrin films to 400 K for 10 sec and for 1 h.

Figure 4b–c show the corresponding images after this annealing step, measured at RT. We initially observed no change in the phases. Long heating, on the other hand, results in the loss of the stripe phase, leaving the square phase and a disordered phase on the surface. Finally, we annealed the adsorbed layers on Cu(111) to 450 K for 20 min. Figure S3 shows the STM images acquired at RT after the annealing process. Remarkably, no ordered square lattice or stripe phase is observed anymore. We observed only a disordered phase. We tentatively assign our observations to a dehydrogenation process within the porphyrin yielding the formation of new intramolecular C–C bonds between the isoindole and the phenyl groups (see refs.^[20b,29,31] and references therein).

2H-diTTBP(x)BPs on Cu(110)

As a final step, we investigated the adsorption and reaction behavior of 2H-diTTBP(x)BPs on Cu(110). This surface is characterized by close-packed Cu rows along the $[1\bar{1}0]$ direction, which yield a unidirectional corrugation. Its open structure is expected to make the surface more reactive than Ag(111) or Cu(111), and it has been therefore also selected as a template substrate.^[20c,32] Sub-monolayer coverage porphyrin films (total surface coverage of $\sim 40\%$) were deposited onto the sample at RT, and measurements were carried out also at RT. Additional measurements were performed after annealing the sample to 400 or 450 K, and subsequent cooling down to RT.

Figure 7a shows the corresponding STM images after deposition at RT. In the overview image (left) and close-up image (right), we observe no long-range ordered phases, but dispersed individual molecules or short linear chains, composed of two to three molecules, at the step edges and on terraces. The chains are aligned along the $[1\bar{1}0]$ direction of the substrate. We attribute our observations to the interaction of the nitrogen atoms of the downward bent isoindole or pyrrole groups, which get closer to the surface on the comparably rough, trough-like Cu(110) surface, leading to specifically favored adsorption sites. The observation of only individual molecules or small ensembles indicates that these specific adsorption sites impose a lateral distance of the molecules, which does not fit to the ordered phases observed on Cu(111), which are stabilized via the lateral van der Waals forces between neighboring molecules.^[20c,d,33] For too large ensembles, the energetic costs for occupying non-optimum adsorption sites cannot be overcompensated by the energy gain due to attractive lateral interactions.

The molecules on Cu(110) are found in two conformations in Figure 7. The first displays four nearly quadratically arranged protrusions (indicated by white circles). The second is a peculiar rectangular shape with six protrusions (indicated by rectangles), with four dim protrusions at the edges and two dim or bright protrusions in the center of the molecule. This appearance is clearly different from the appearance of the molecules in the stripe phase on Cu(111). It is, however, similar to the appearance of 2H-tetraphenylporphyrins (2H-TTP) and 2H-tetranaphthylporphyrins (2H-TNP) on Cu(111),^[23,34] which both

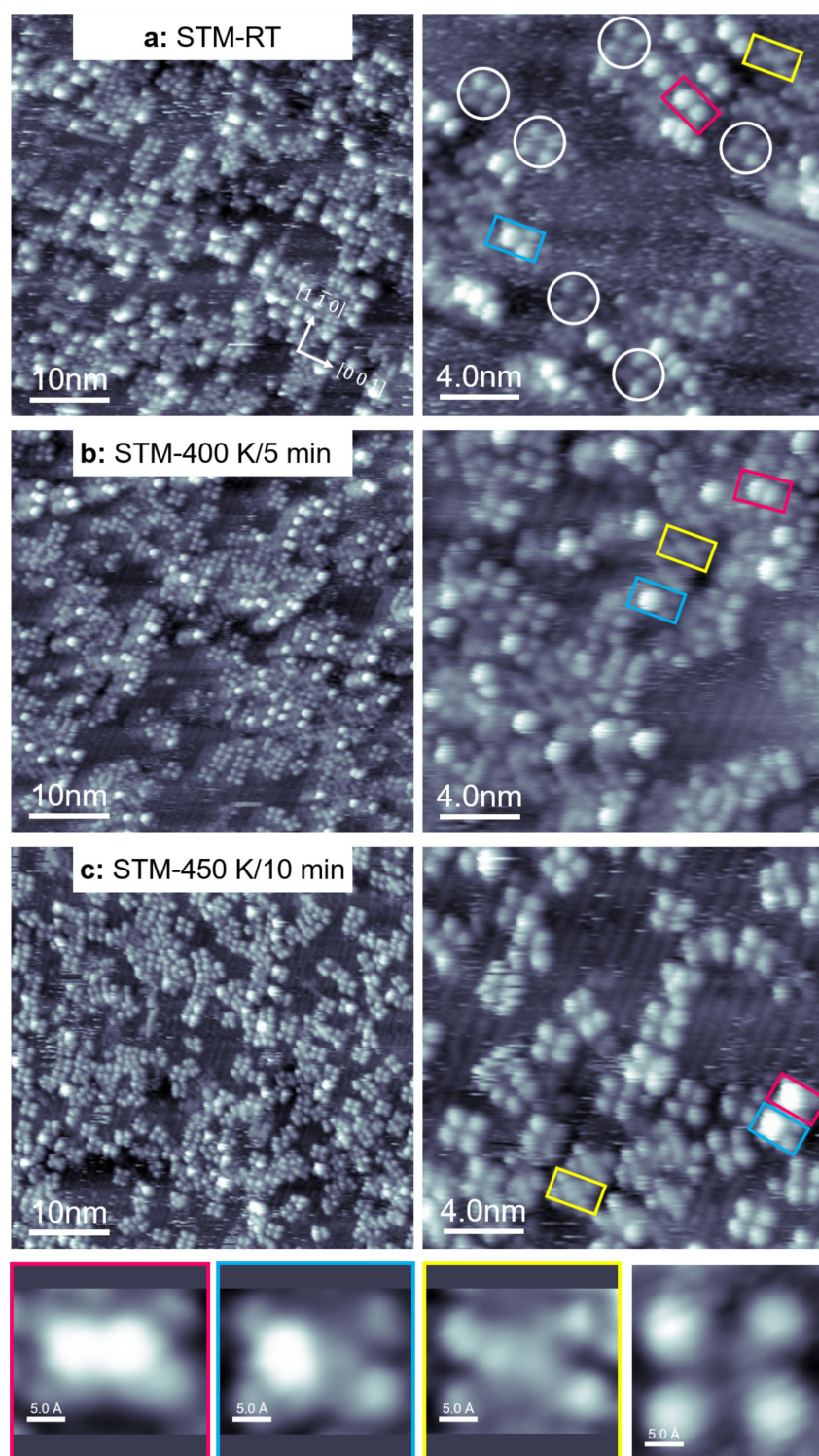


Figure 7. STM images of 2H-diTTBP(x)BPs on Cu(110), as an overview (left, $50 \times 50 \text{ nm}^2$), with close-up (right, $20 \times 20 \text{ nm}^2$), and with high resolution (bottom left three, $2.5 \times 1.86 \text{ nm}^2$; bottom-right, $2.5 \times 2.5 \text{ nm}^2$), measured at RT. a) Deposition at RT reveals isolated molecules and the formation of short isolated 1D chains. b) After annealing to 400 K for 5 min and c) 450 K for 10 min, the molecular appearance remains unchanged. The close-up STM images and the high-resolution images reveal individual isolated molecules with two conformations (measured at RT): a quadratic arrangement of four lobes (white circle or frame) and rectangular arrangement with six lobes (colored frames). The latter is assigned to an “inverted” structure and has three different appearances (indicated by different colors). For more details, see text. The white arrows indicate the close-packed Cu(110) substrate directions. The STM images were measured with U_{bias} between -1.28 and $+1.25$ V and I_{set} between 195 and 197 pA; for details see Table S1.

have an inverted structure with two pyrrole groups oriented nearly perpendicular to the surface. From this similarity, we propose an inverted structure also for 2H-diTTBP(x)BPs on Cu(110).

From the high-resolution images in Figure 7 (bottom row) and Figure 8a, 8b, and 8c, we can further analyze the two different conformations of the 2H-diTTBP(x)BPs. For the inverted conformation, we observe three different appearances of the two central protrusions (indicated by a red, blue, or yellow frames), which we tentatively can correlate with the number of isoindole groups. The assignment is illustrated in Figure 8, where the STM images are overlaid by scaled molecular models. In all of them, a bright central protrusion is assigned to a vertical isoindole group and a dim protrusion to a vertical pyrrole group (the horizontal isoindole or pyrrole groups cannot

be identified): TWO bright central protrusions (red frame) are assigned to $x=4$ (a1), 3 (a2), or 2-trans (a3), with two vertical isoindole groups, ONE bright central protrusion (blue frame) to $x=3$ (b1), $x=2$ -cis (b2), or $x=1$ (b3), with one vertical isoindole group, ZERO bright central protrusions (yellow frame) are assigned to $x=2$ -trans (c1), 1 (c2), or 0 (c3), with no vertical isoindole group; notably for pure 2H-tetrakis(3,5-di-*tert*-butyl)phenylporphyrin (2H-diTTBPP), that is, the molecule without an isoindole group ($x=0$), a different appearance has been observed.^[35]

The appearance with four (nearly) quadratically arranged protrusions for the individual molecules (white frames) is quite different from the crown-shape appearance with four protrusions in the square phases on Ag(111) and Cu(111), which are attributed to upward bent isoindole or pyrrole groups. Here,

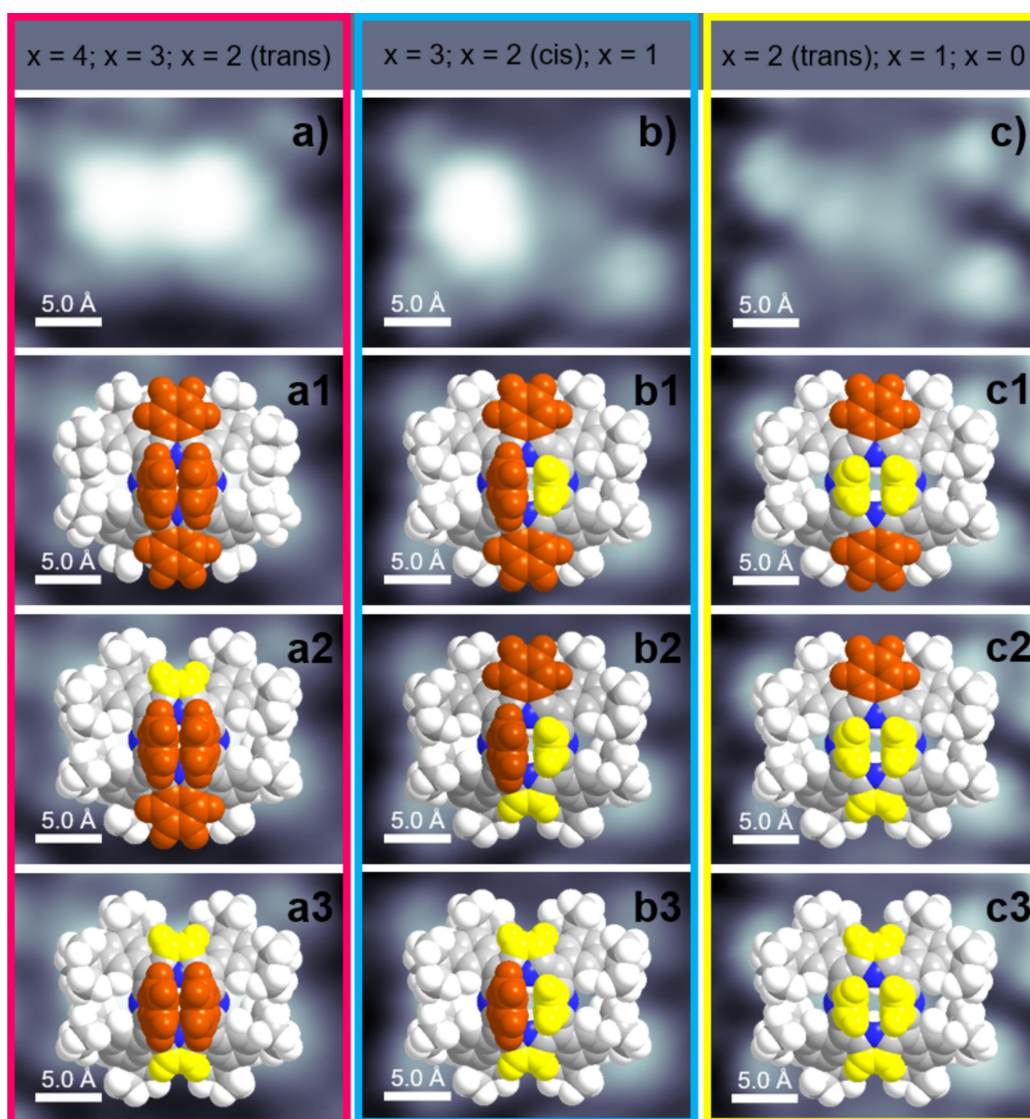


Figure 8. Cutouts ($2.5 \times 1.86 \text{ nm}^2$; same high resolution images as in bottom row in Figure 7, measured at RT) of the inverted structures in the STM images of 2H-diTTBP(x)BPs on Cu(110) (a–c), along with superimposed scaled molecular models of individual molecules with TWO bright protrusions (a1–a3: left/red frame; $x=4$, 3, or 2-trans), ONE bright protrusion (b1–b3: middle/blue frame; $x=3$, 2-cis, or 1), and ZERO bright protrusions (c1–c3: right/yellow frame; $x=2$ -trans, 1, or 0), to illustrate the different conformations. Isoindole groups are depicted in orange, and pyrrole groups are depicted in yellow. The individual molecules are marked with differently colored frames, with the same color code as used in Figure 7; for more details, see text.

the protrusions are separated by 10 to 12 Å, that is, by about twice the distance than for the “crown-shape” conformation. We thus tentatively assign the structure with four quadratically arranged protrusions to a quite different conformation, in which the isoindole and pyrrole groups are in the plane of the macrocycle and all phenyl groups bent upward and rotated, such that one of the bulky di-*tert*-butyl groups points upward. With this conformation, the four bright protrusions would be due to the upward bent *tert*-butyl phenyl groups. Notably, the appearance of the quadratically arranged protrusions in Figure 7 slightly varies from molecule to molecule. Thus, an unequivocal assignment to the different 2H-diTTBP(x)BPs species is not possible, and our interpretation of the appearance with four quadratically arranged protrusions in the STM images must remain speculative. We also cannot draw conclusions concerning potential self-metalation of the molecule with Cu adatoms: While for Cu(111) self-metalation typically leads to the formation of long-range ordered island of the metalloporphyrins,^[9a,27a,29] this is not the case on Cu(110), where both 2H-diTTBP and Cu-diTTBP is observed as individual isolated molecules.^[35]

To probe the stability of conformations and short chains, we annealed the deposited porphyrin films to 400 K for 5 min and to 450 K for 10 min, respectively. Figure 7b and 7c show the corresponding overview and close-up images. Overall, we again observe dispersed short linear 1D chains aligned along the [1 $\bar{1}$ 0] direction of the substrate coexisting with individual isolated molecules, with no significant transformations. The molecules in both conformations seem to be intact and thermodynamically stable up to 450 K.

Conclusions

We investigated the adsorption behavior of the mixture of 2H-tetrakis-(3, 5-di-*tert*-butylphenyl)(x)benzoporphyrins (2H-diTTBP(x)BPs) on Ag(111), Cu(111), and Cu(110) surfaces by scanning tunneling microscopy at room temperature. The mixture contained six different 2H-diTTBP(x)BPs with $x=0, 1, 2$ -cis, 2-trans, 3, and 4, as obtained from synthesis. For the three surfaces, we obtain a quite different adsorption behavior concerning long-range order and intramolecular conformation of the porphyrins. Notably, on all surfaces, high resolution STM images allow for identifying the different 2H-diTTBP(x)BPs.

On Ag(111), the adsorption of the mixture results in a long-range ordered two-dimensional square phase, which is stable upon heating to 400 K. The individual molecules appear a four quadratically arranged dim or bright protrusions, which are assigned to upward bent isoindole or pyrrole groups in a so-called crown conformation. On Cu(111), the same square phase coexists with a stripe phase; in the latter, the molecules have a rectangular shape with two parallel groups of three protrusion, which reflect a saddle-shape conformation. Heating to 400 K leads to the loss of the stripe phase but leaves the square phase intact. The observation of the same square phase of the mixture of 2H-diTTBP(x)BPs on both surfaces indicates that the long-range order is stabilized by the outer periphery of the

molecules and not by the substrate or the number of isoindole groups.

In contrast, on Cu(110), 2H-diTTBP(x)BPs adsorb as isolated molecules or dispersed short (two to three molecules long) one-dimensional chains along the [1 $\bar{1}$ 0] substrate direction that coexist with isolated individual immobile molecules; this structure remains intact up to 450 K. The individual molecules display two conformations. The first is a peculiar rectangular shape with four dim outer protrusions and two dim or bright central protrusions, indicative of an “inverted” conformation of the molecules. The second displays four (nearly) quadratically arranged protrusions for the individual molecules, and is quite different from the crown-shape appearance on Ag(111) and Cu(111); we tentatively attribute it to a structure, in which the isoindole and pyrrole groups are in the plane of the macrocycle and all phenyl groups are bent upward and rotated such that one of the bulky di-*tert*-butyl groups points upward.

The formation and lateral stabilization of 2D supramolecular structures on Ag(111) and Cu(111), as well as 1D short chains on Cu(110) are attributed to van der Waals interactions between the *tert*-butyl possibly phenyl groups of the neighboring molecules. The different conformations observed on the three surfaces are assigned to the different degree of interaction of the iminic nitrogen atoms of the isoindole and pyrrole groups with the substrate atoms. The thermal stability of the crown conformation for the square phases on Ag(111) and Cu(111), and the isolated immobile molecules on Cu(110) indicates the absence of a reaction under the investigated conditions. In contrast, the disappearance of the saddle-shape conformation of the stripe phase on Cu(111) upon longer annealing at 400 K indicates a reaction, the nature of which is, however, difficult to identify. A simple self-metalation of 2H-porphyrins to Cu-porphyrins with substrate adatoms appears unlikely, as metalated porphyrins typically show pronounced island formation, which is not observed after heating. Finally, the stability of the “inverted” structure on Cu(110) proves the absence of a self-metalation, since the inverted structure is not compatible with a central fourfold coordinated metal center of a metalloporphyrin. For the molecules displaying four (nearly) quadratically arranged protrusions metalation cannot be ruled out. Further insights possibly could be obtained by extensive DFT calculations to understand the different structures and conformations on the three surfaces, which is however, out of the scope of this study.

Experimental

All experiments, sample preparations, and STM measurements were performed in an ultrahigh vacuum (UHV) system with a base pressure in the low 10^{-10} mbar regime. The preparation of the Ag(111), Cu(111), and Cu(110) surfaces was done by sequential cycles of Ar⁺ ion bombardment (600 or 700 eV) followed by annealing at 850 K. STM was performed using an RHK UHV VT STM 300 operated at RT, with RHK SPM 100 electronics. All STM images were obtained with a manually cut Pt/Ir tip, in constant current mode. The denoted bias voltages refer to the sample. The STM images were processed with the WSxM software. For noise reduction, moderate filtering (background subtraction, Gaussian

smoothing) was applied.^[24] The 2H-diTTBP(x)BPs molecules were deposited onto the substrates held at RT using a home-built Knudsen cell with the crucible at 651–662 K. The STM measurements were typically initiated 1–2 h after preparation.

Notes

The authors declare no competing financial interest.

Acknowledgements

The authors gratefully acknowledge funding by the German Research Foundation (DFG) through RTG 2861 (project number 491865171) at the Friedrich-Alexander-Universität Erlangen-Nürnberg and the TU Dresden, and SFB 953 (project number 182849149) at the Friedrich-Alexander-Universität Erlangen-Nürnberg. Open Access funding enabled and organized by Projekt DEAL.

Conflict of Interests

The authors declare no conflict of interest.

Data Availability Statement

The data that support the findings of this study are available from the corresponding author upon reasonable request.

Keywords: benzoporphyrin · isoindole groups · 2H-diTTBP(x)BPs · scanning tunneling microscopy · self-assembly

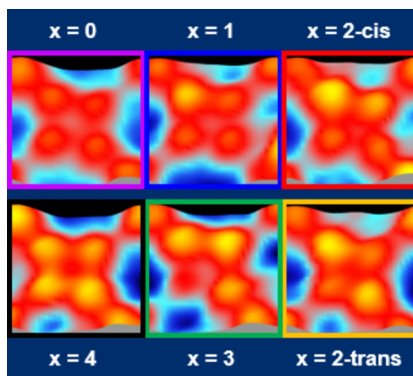
- [1] a) C. Joachim, J. K. Gimzewski, A. Aviram, *Nature* **2000**, *408*, 541–548; b) M. Ratner, *Nat. Nanotechnol.* **2013**, *8*, 378–381.
- [2] a) J. K. Gimzewski, C. Joachim, *Science* **1999**, *283*, 1683–1688; b) H. Marbach, H.-P. Steinrück, *Chem. Commun.* **2014**, *50*, 9034–9048; c) H. Marbach, *Acc. Chem. Res.* **2015**, *48*, 2649–2658; d) W. Auwärter, D. Écija, F. Klappenberger, J. V. Barth, *Nat. Chem.* **2015**, *7*, 105–120; e) K. Diller, A. C. Papageorgiou, F. Klappenberger, F. Allegretti, J. V. Barth, W. Auwärter, *Chem. Soc. Rev.* **2016**, *45*, 1629–1656.
- [3] a) S. Ditze, M. Stark, M. Drost, F. Buchner, H.-P. Steinrück, H. Marbach, *Angew. Chem. Int. Ed.* **2012**, *51*, 10898–10901; b) F. Klappenberger, A. Weber-Bargioni, W. Auwärter, M. Marschall, A. Schiffrin, J. Barth, *J. Chem. Phys.* **2008**, *129*, 214702; c) S. Ditze, M. Stark, F. Buchner, A. Aichert, N. Jux, N. Luckas, A. Görling, W. Hieringer, J. Hornegger, H.-P. Steinrück, H. Marbach, *J. Am. Chem. Soc.* **2014**, *136*, 1609–1616.
- [4] Y. Wada, M. Tsukada, M. Fujihira, K. Matsushige, T. Ogawa, M. Haga, S. Tanaka, *Jpn. J. Appl. Phys.* **2000**, *39*, 3835.
- [5] T. Jung, R. Schlittler, J. Gimzewski, *Nature* **1997**, *386*, 696–698.
- [6] a) I. Fleming, *Nature* **1967**, *216*, 151–152; b) C. E. Castro, *J. Theor. Biol.* **1971**, *33*, 475–490.
- [7] A. R. Battersby, *Nat. Prod. Rep.* **2000**, *17*, 507–526.
- [8] a) A. Zampetti, A. Minotto, F. Cacialli, *Adv. Funct. Mater.* **2019**, *29*, 1807623; b) C. B. Winkelmann, I. Iónica, X. Chevalier, G. Royal, C. Bucher, V. Bouchiat, *Nano Lett.* **2007**, *7*, 1454–1458; c) R. n. Flores-Sánchez, F. Gámez, T. n. Lopes-Costa, J. M. Pedrosa, *ACS Omega* **2020**, *5*, 6299–6308; d) K. Kurlekar, A. Anjali, S. Sonalin, P. M. Imran, S. Nagarajan, *ACS Appl. Electron. Mater.* **2020**, *2*, 3402–3408.
- [9] a) R. Adhikari, G. Sigleithmaier, M. Gurrath, M. Meusel, J. Kuliga, M. Lepper, H. Hölzel, N. Jux, B. Meyer, H.-P. Steinrück, H. Marbach, *Chemistry—A European Journal* **2020**, *26*, 13408–13418; b) M. Lepper, J. Köbl, L. Zhang, M. Meusel, H. Hölzel, D. Lungerich, N. Jux, A. de Siervo, B. Meyer, H.-P. Steinrück, H. Marbach, *Angew. Chem. Int. Ed.* **2018**, *57*, 10074–10079.
- [10] M. Stark, S. Ditze, M. Drost, F. Buchner, H.-P. Steinrück, H. Marbach, *Langmuir* **2013**, *29*, 4104–4110.
- [11] M. Stark, S. Ditze, M. Lepper, L. Zhang, H. Schlott, F. Buchner, M. Röckert, M. Chen, O. Lytken, H.-P. Steinrück, H. Marbach, *Chem. Commun.* **2014**, *50*, 10225–10228.
- [12] J. Kuliga, L. Zhang, M. Lepper, D. Lungerich, H. Hölzel, N. Jux, H.-P. Steinrück, H. Marbach, *Phys. Chem. Chem. Phys.* **2018**, *20*, 25062–25068.
- [13] J. M. Gottfried, *Surf. Sci. Rep.* **2015**, *70*, 259–379.
- [14] C. M. B. Carvalho, T. J. Brocksom, K. T. De Oliveira, *Chem. Soc. Rev.* **2013**, *42*, 3302–3317.
- [15] a) C. Borek, K. Hanson, P. I. Djurovich, M. E. Thompson, K. Aznavour, R. Bau, Y. Sun, S. R. Forrest, J. Brooks, L. Michalski, *Angew. Chem. Int. Ed.* **2007**, *46*, 1109–1112; b) J. R. Sommer, A. H. Shelton, A. Parthasarathy, I. Ghiviriga, J. R. Reynolds, K. S. Schanze, *Chem. Mater.* **2011**, *23*, 5296–5304; c) K. R. Graham, Y. Yang, J. R. Sommer, A. H. Shelton, K. S. Schanze, J. Xue, J. R. Reynolds, *Chem. Mater.* **2011**, *23*, 5305–5312.
- [16] L. Hutter, B. Müller, K. Koren, S. Borisov, I. Klimant, *J. Mater. Chem. C* **2014**, *2*, 7589–7598.
- [17] F. Ménard, V. Sol, C. Ringot, R. Granet, S. Alves, C. Le Morvan, Y. Queneau, N. Ono, P. Krausz, *Bioorg. Med. Chem.* **2009**, *17*, 7647–7657.
- [18] a) S. Aramaki, Y. Sakai, N. Ono, *Appl. Phys. Lett.* **2004**, *84*, 2085–2087; b) P. B. Shea, J. Kanicki, N. Ono, *J. Appl. Phys.* **2005**, *98*, 014503; c) P. B. Shea, J. Kanicki, L. R. Pattison, P. Petroff, M. Kawano, H. Yamada, N. Ono, *J. Appl. Phys.* **2006**, *100*, 034502; d) P. B. Shea, C. Chen, J. Kanicki, L. R. Pattison, P. Petroff, H. Yamada, N. Ono, *Appl. Phys. Lett.* **2007**, *90*, 233107.
- [19] Y. Matsuo, Y. Sato, T. Niinomi, I. Soga, H. Tanaka, E. Nakamura, *J. Am. Chem. Soc.* **2009**, *131*, 16048–16050.
- [20] a) J. Brox, R. Adhikari, M. Shaker, M. Ruppel, N. Jux, H. Marbach, S. Jaekel, H.-P. Steinrück, *Surf. Sci.* **2022**, *720*, 122047; b) R. Adhikari, J. Kuliga, M. Ruppel, N. Jux, H. Marbach, H.-P. Steinrück, *J. Phys. Chem. C* **2021**, *125*, 7204–7212; c) L. Zhang, M. Lepper, M. Stark, T. Menzel, D. Lungerich, N. Jux, W. Hieringer, H.-P. Steinrück, H. Marbach, *Phys. Chem. Chem. Phys.* **2017**, *19*, 20281–20289; d) M. Lepper, L. Zhang, M. Stark, S. Ditze, D. Lungerich, N. Jux, W. Hieringer, H.-P. Steinrück, H. Marbach, *J. Phys. Chem. C* **2015**, *119*, 19897–19905; e) L. Zhang, M. Lepper, M. Stark, D. Lungerich, N. Jux, W. Hieringer, H.-P. Steinrück, H. Marbach, *Phys. Chem. Chem. Phys.* **2015**, *17*, 13066–13073.
- [21] M. Ruppel, D. Lungerich, S. Sturm, R. Lippert, F. Hampel, N. Jux, *Chem. A Eur. J.* **2020**, *26*, 3287–3296.
- [22] M. Ruppel, L.-P. Gazetas, D. Lungerich, F. Hampel, N. Jux, *J. Org. Chem.* **2020**, *85*, 7781–7792.
- [23] M. Lepper, J. Köbl, T. Schmitt, M. Gurrath, A. de Siervo, M. A. Schneider, H.-P. Steinrück, B. Meyer, H. Marbach, W. Hieringer, *Chem. Commun.* **2017**, *53*, 8207–8210.
- [24] I. Horcas, R. Fernández, J. Gomez-Rodriguez, J. Colchero, J. Gómez-Herrero, A. Baro, *Rev. Sci. Instrum.* **2007**, *78*, 013705.
- [25] a) F. Buchner, I. Kellner, W. Hieringer, A. Görling, H.-P. Steinrück, H. Marbach, *Phys. Chem. Chem. Phys.* **2010**, *12*, 13082–13090; b) F. Buchner, V. Schwald, K. Comanici, H.-P. Steinrück, H. Marbach, *ChemPhysChem* **2007**, *8*, 241–243; c) M. Lepper, T. Schmitt, M. Gurrath, M. Raschmann, L. Zhang, M. Stark, H. Hölzel, N. Jux, B. Meyer, M. A. Schneider, H.-P. Steinrück, H. Marbach, *J. Phys. Chem. C* **2017**, *121*, 26361–26371.
- [26] J. Brede, M. Linares, S. Kuck, J. Schwöbel, A. Scarfato, S.-H. Chang, G. Hoffmann, R. Wiesendanger, R. Lensen, P. H. Kouwer, *Nanotechnology* **2009**, *20*, 275602.
- [27] a) F. Buchner, E. Zillner, M. Röckert, S. Gläsel, H.-P. Steinrück, H. Marbach, *Chem. A Eur. J.* **2011**, *17*, 10226–10229; b) F. Buchner, J. Xiao, E. Zillner, M. Chen, M. Röckert, S. Ditze, M. Stark, H.-P. Steinrück, J. M. Gottfried, H. Marbach, *J. Phys. Chem. C* **2011**, *115*, 24172–24177.
- [28] a) A. Weber-Bargioni, W. Auwärter, F. Klappenberger, J. Reichert, S. Lefrançois, T. Strunskus, C. Wöll, A. Schiffrin, Y. Pennec, J. V. Barth, *ChemPhysChem* **2008**, *9*, 89–94; b) K. Diller, F. Klappenberger, M. Marschall, K. Hermann, A. Nefedov, C. Wöll, J. Barth, *J. Chem. Phys.* **2012**, *136*, 014705; c) T. Yokoyama, S. Yokoyama, T. Kamikado, S. Mashiko, *J. Chem. Phys.* **2001**, *115*, 3814–3818.
- [29] J. Xiao, S. Ditze, M. Chen, F. Buchner, M. Stark, M. Drost, H.-P. Steinrück, J. M. Gottfried, H. Marbach, *J. Phys. Chem. C* **2012**, *116*, 12275–12282.

- [30] M. Xi, M. X. Yang, S. K. Jo, B. E. Bent, P. Stevens, *J. Chem. Phys.* **1994**, *101*, 9122–9131.
- [31] G. Di Santo, C. Castellarin-Cudia, M. Fanetti, B. Taleatu, P. Borghetti, L. Sangaletti, L. Floreano, E. Magnano, F. Bondino, A. Goldoni, *J. Phys. Chem. C* **2011**, *115*, 4155–4162.
- [32] M. Oehzelt, L. Grill, S. Berkebile, G. Koller, F. P. Netzer, M. G. Ramsey, *ChemPhysChem* **2007**, *8*, 1707–1712.
- [33] W. Auwärter, A. Weber-Bargioni, A. Riemann, A. Schiffrin, O. Gröning, R. Fasel, J. Barth, *J. Chem. Phys.* **2006**, *124*, 194708.
- [34] J. Kuliga, S. Massicot, R. Adhikari, M. Ruppel, N. Jux, H.-P. Steinrück, H. Marbach, *ChemPhysChem* **2020**, *21*, 423–427.
- [35] L. Zhang, M. Lepper, M. Stark, R. Schuster, D. Lungerich, N. Jux, H.-P. Steinrück, H. Marbach, *Chem. A Eur. J.* **2016**, *22*, 3347–3354.

Manuscript received: May 19, 2023
Revised manuscript received: June 21, 2023
Accepted manuscript online: June 21, 2023
Version of record online: ■ ■, ■ ■

RESEARCH ARTICLE

A mixture of six 2H-tetrakis-(3, 5-di-*tert*-butylphenyl)(*x*)benzoporphyrins (2H-diTTBP(*x*)BPs, *x* = 0, 1, 2-*cis*, 2-*trans*, 3, and 4) on Ag(111) as observed in high-resolution scanning tunneling microscopy at room temperature.



*R. Adhikari, Dr. J. Brox, S. Massicot, Dr. M. Ruppel, Prof. Dr. N. Jux, Dr. H. Marbach, Prof. Dr. H.-P. Steinrück**

1 – 15

Structure and Conformation of Individual Molecules upon Adsorption of a Mixture of Benzoporphyrins on Ag(111), Cu(111), and Cu(110) Surfaces

